Cognitive Interference Suppression for Low Complexity UWB Transceivers

Christoph Steiner and Armin Wittneben
Communication Technology Laboratory, ETH Zurich, CH-8092, Switzerland
Email: {steinech,wittneben}@nari.ee.ethz.ch

***Abstract*— Interference suppression techniques for low complexity Ultra-Wideband transceivers using pulse position modulation and energy detection receivers are proposed and evaluated. A theoretical framework is introduced, which enables the optimization of pulse shapes and energy detection integration windows based on a signal-to-interference-and-noise ratio criterion. Furthermore, the framework allows to incorporate statistical channel knowledge into the optimization problem. The effect of the proposed interference suppression techniques on BER performance is demonstrated by computer simulations.**

I. Introduction

Wireless sensor networks (WSN) and body area networks (BAN) are two of the main expected technological breakthroughs supported by wireless communication. However, the application of such wireless networks is still impeded by battery autonomy of the nodes, medium access and networking issues, coexistence with other wireless systems, and hardware complexity. A joint optimization within this large design space is computationally intractable and different features are mutually exclusive. For example, low complexity non-coherent (nonlinear) receiver structures are more vulnerable to interference than coherent receivers, which have in turn a higher power consumption due to increased complexity. Ultra-Wideband (UWB) has proven to be the technology of choice to combat some of the issues mentioned above [1]. Furthermore, UWB has an inherent potential to fulfill key requirements of cognitive radio, where nodes adapt their communication behavior and system parameters to the environment [2]. Adaptable pulse shapes and scalable data rates are two prominent cognitive features, which are supported by UWB systems.

In this work, we address the coexistence problem and optimize the transmit pulse shape and the integration window of an energy detection receiver based on the knowledge of the power spectral density (PSD) of interference and noise. For pulse shaping, the transmitter must have information about the interference on the receiver side. However, in WSN and BAN scenarios it is likely that transmitter and receiver exhibit the same interference. Moreover, the spectral occupation of common wireless systems like WLAN, UMTS, or GSM are known a-priori, which means that only the interference power must be estimated at the receiver and disseminated to the transmitter.

A pulse shaping method based on finite impulse response filter design is proposed in [3]. Although the resulting pulses fit into the FCC mask and can avoid narrowband interference, this method is neither designed to exploit statistical channel knowledge nor to account for different integration windows of an energy detection receiver. Both features are accounted for in the proposed pulse shaping approach.

The impact of interference on energy detection receivers with rectangular integration window is investigated in [4], where it is shown that for wideband interferers the quadratic interference term is limiting the performance. It is shown in this work that the integration window can be adapted such that this quadratic part is also suppressed. In [5] the authors present a multichannel system model of an energy detection receiver with a bank of autocorrelation blocks that is able to mitigate interference at increased receiver complexity.

Notation: $*$, $\odot$, $(\cdot)^T$, and $\mathrm{E}_x\{\cdot\}$ denote convolution, Hadamard product, transposition, and expectation with respect to the random variable x, respectively.

II. Discrete Time System Model

We consider a communication scenario according to Fig. 1. The transmitter employs binary pulse position modulation (PPM) and the receiver uses energy detection. The received

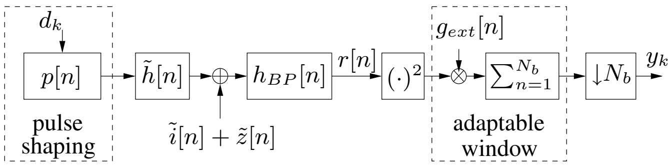

Fig. 1. Discrete time system model.

signal $r[n]$ after the bandpass and before the squaring device is given by

$$r[n] = \sum_k p\left[n - kN_b - d_k N_{ppm}\right] * \tilde{h}[n] * h_{BP}[n] + \left(\tilde{i}[n] + \tilde{z}[n]\right) * h_{BP}[n], \quad (1)$$

where N_b and N_{ppm} are the number of samples for one bit and one PPM slot, respectively. In the following, N_{ppm} is set to $N_b/2$ assuming that N_b is an even number. The data bits $d_k \in \{0, 1\}$ are equally likely and independent. Expression (1) can be simplified by considering bit $k = 0$ and by convolving channel $\tilde{h}[n]$, interference $\tilde{i}[n]$, and noise $\tilde{z}[n]$ with the bandpass $h_{BP}[n]$ yielding $h[n]$, $i[n]$, and $z[n]$. Using these notational simplifications, the received signal is given by

$$r[n] = p[n - d_0 N_{ppm}] * h[n] + i[n] + z[n].$$

It is assumed that $h[n] = \tilde{h}[n] * h_{BP}[n]$ has N_h non-zero samples and the transmit pulse $p[n]$ has N_p non-zero samples. This means that the received pulse $p[n] * h[n]$ has in total $N_r = N_p + N_h - 1$ non-zero samples. In order to avoid interslot and intersymbol interference, we require $N_r \leq N_{ppm}$. The noise samples $z[n]$ and interference samples $i[n]$ are assumed to be Gaussian distributed with zero mean and autocorrelation functions $R_Z[m]$ and $R_I[m]$, respectively. Furthermore, it is assumed that channel, noise, and interference are independent.

The convolution of $p[n]$ with the channel $h[n]$ can be written as a multiplication with matrix $\mathbf{H}$, which has a Toeplitz structure, dimensions $N_b \times N_b$, and collects the shifted and zero-padded versions of $[h[1], h[2], \ldots, h[N_h], 0, \ldots, 0]$ on its columns. Thus, the input-output relation for one bit in matrix notation using column vectors of length N_b is given by

$$\mathbf{r} = \mathbf{H}\mathbf{p} + \mathbf{i} + \mathbf{z},$$

where the vector $\mathbf{p}$ consists of the transmit pulse of length N_p and $N_b - N_p$ zeros.

III. Energy Detection Receiver

The energy detection receiver calculates the decision variable y using the integration window $\mathbf{g}_{ext}^T = [\mathbf{g}^T, -\mathbf{g}^T]$ of length N_b according to

$$y = \mathbf{g}_{ext}^T (\mathbf{r} \odot \mathbf{r}) = s + i_q + z_q + i_s + z_s + z_i.$$

If $y > 0$, it decides in favor of bit 0, otherwise it decides for bit 1. Besides the signal contribution s, there exist five terms due to the squaring operation which degrade the detection performance. The terms i_q and z_q are the squared interference and noise terms, i_s is the signal times interference term, z_s is the signal times noise term, and z_i is the interference times noise term. It can be shown that all five terms have zero mean and that they are mutually uncorrelated. This follows from the zero mean property, stationarity, and Gaussianity of the random processes $i[n]$ and $z[n]$, and the independence of $h[n]$, $i[n]$, and $z[n]$.

The ratio of the average squared signal energy to the average squared noise and interference energy depends on the transmit pulse and the integration window and is defined as

$$\begin{aligned}\mathrm{SINR}(\mathbf{p}, \mathbf{g}) &= \frac{\mathrm{E}_h\left\{s^2\right\}}{\mathrm{E}_{h,i,z}\left\{(i_q + z_q + i_s + z_s + z_i)^2\right\}} \\ &= \frac{\mathrm{E}_h\left\{s^2\right\}}{\mathrm{E}_i\{i_q^2\} + \mathrm{E}_z\{z_q^2\} + \mathrm{E}_{h,i}\{i_s^2\} + \mathrm{E}_{h,z}\{z_s^2\} + \mathrm{E}_{i,z}\{z_i^2\}}. \end{aligned} \quad (2)$$

The second line follows from the fact that all terms in the denominator are mutually uncorrelated. The SINR expression in (2) is an approximation for the expected SINR, since the expectation over the channel is taken separately for numerator and denominator. This simplification is required, because the problem is mathematically intractable otherwise. Furthermore, the decision variable y is not Gaussian distributed, which implies maximizing (2) for a given channel realization does not necessarily minimize bit error probability. However, it is shown in Section VI that performance gains can be obtained by maximizing (2), if the performance is limited by interference.

In Section IV the transmit pulse $\mathbf{p}^\star$ that maximizes (2) for a given integration window is derived and in Section V the optimal integration window $\mathbf{g}^\star$ for the optimized transmit pulse is found. By iterating over these two steps a joint optimization of $\mathbf{p}$ and $\mathbf{g}$ can be performed, which is, however, outside the scope of this paper.

IV. Transmit Pulse Optimization

The vector $\mathbf{p}$ influences the terms i_s and z_s given by

$$i_s = 2\mathbf{g}_{ext}^T (\mathbf{H}\mathbf{p} \odot \mathbf{i}) \text{ and } z_s = 2\mathbf{g}_{ext}^T (\mathbf{H}\mathbf{p} \odot \mathbf{z}).$$

The variance of i_s and z_s for a given integration window $\mathbf{g}_{ext}$ can be written as

$$\mathrm{E}_{h,i}\{i_s^2\} = 4\mathbf{p}^T \left(\mathrm{E}_h\{\mathbf{H}^T \left[(\mathbf{g}_{ext}\mathbf{g}_{ext}^T) \odot \mathbf{R}_I\right] \mathbf{H}\}\right) \mathbf{p} = \mathbf{p}^T \mathbf{B}_I \mathbf{p},$$
$$\mathrm{E}_{h,z}\{z_s^2\} = 4\mathbf{p}^T \left(\mathrm{E}_h\{\mathbf{H}^T \left[(\mathbf{g}_{ext}\mathbf{g}_{ext}^T) \odot \mathbf{R}_Z\right] \mathbf{H}\}\right) \mathbf{p} = \mathbf{p}^T \mathbf{B}_Z \mathbf{p},$$

where the correlation matrices $\mathbf{R}_I$ and $\mathbf{R}_Z$ depend on the autocorrelation functions $R_I[m]$ and $R_Z[m]$. For example, the (i, j)-th element of $\mathbf{R}_I$ is given by $R_I[i - j]$. Since the autocorrelation functions are symmetric around zero, also the matrices $\mathbf{R}_I$ and $\mathbf{R}_Z$ are symmetric. Furthermore, $\mathbf{p}$ influences the received signal energy s, which is given by $s = \mathbf{g}_{ext}^T (\mathbf{H}\mathbf{p} \odot \mathbf{H}\mathbf{p})$. The expected value of s^2 can be written as

$$\begin{aligned}\mathrm{E}_h\left\{s^2\right\} &= \mathbf{g}_{ext}^T \mathrm{E}_h\left\{(\mathbf{H}\mathbf{p} \odot \mathbf{H}\mathbf{p})(\mathbf{H}\mathbf{p} \odot \mathbf{H}\mathbf{p})^T\right\} \mathbf{g}_{ext} \\ &= \mathbf{g}_{ext}^T \mathbf{Q} \mathbf{g}_{ext}. \end{aligned} \quad (3)$$

The matrix $\mathbf{Q}$ has dimensions $N_b \times N_b$. The (i, j)-th element of this matrix is given by

$$\begin{aligned} Q_{i,j} &= \mathbf{p}^T \mathrm{E}_h\left\{\mathbf{h}_i \mathbf{h}_i^T\right\} \mathbf{p} \cdot \mathbf{p}^T \mathrm{E}_h\left\{\mathbf{h}_j \mathbf{h}_j^T\right\} \mathbf{p} \\ &\quad + 2\mathbf{p}^T \mathrm{E}_h\left\{\mathbf{h}_i \mathbf{h}_j^T\right\} \mathbf{p} \cdot \mathbf{p}^T \mathrm{E}_h\left\{\mathbf{h}_i \mathbf{h}_j^T\right\} \mathbf{p}, \end{aligned}$$

where $\mathbf{h}_i^T$ is the i-th row of $\mathbf{H}$. For this derivation it is assumed that the channel taps are zero-mean Gaussian distributed. The expected values of $\mathbf{h}_i \mathbf{h}_j^T$ depend on the covariance matrix of the channel impulse response. The obtained expression for $\mathrm{E}_h\left\{s^2\right\}$ in (3) is a simple function of $\mathbf{g}_{ext}$ (quadratic form), but a fourth order polynomial in $\mathbf{p}$. Numerical optimization of (2) with respect to $\mathbf{p}$ using (3) turns out to be computationally intractable.

In order to simplify the optimization problem, we use $(\mathrm{E}_h\{s\})^2$ as lower bound for $\mathrm{E}_h\left\{s^2\right\}$. The squared value of the expected signal energy is given by

$$(\mathrm{E}_h\{s\})^2 = \left(\mathbf{p}^T \hat{\mathbf{Q}} \mathbf{p}\right)^2.$$

The matrix $\hat{\mathbf{Q}}$ has dimensions $N_b \times N_b$ and is given by

$$\hat{\mathbf{Q}} = \sum_{n=1}^{N_b} g_{ext}[n] \mathrm{E}_h\left\{\mathbf{h}_n \mathbf{h}_n^T\right\}.$$

The optimal $\mathbf{p}^\star$, which maximizes a lower bound on (2) is calculated by solving the optimization problem stated as

$$\mathbf{p}^\star = \underset{\mathbf{p}:\mathbf{p}^T\mathbf{p}=\text{const}}{\text{argmax}} \frac{\left(\mathbf{p}^T\hat{\mathbf{Q}}\mathbf{p}\right)^2}{\mathbf{p}^T\left(\mathbf{B}_I+\mathbf{B}_Z\right)\mathbf{p}+c},$$

where the constant c is given by

$$c = \mathrm{E}_i\left\{i_q^2\right\} + \mathrm{E}_z\left\{z_q^2\right\} + \mathrm{E}_{i,z}\left\{z_i^2\right\}.$$

The power constraint on $\mathbf{p}$ can be incorporated into the optimization problem by normalizing $\mathbf{p}$ to unit length, which leads to the follwing unconstrained optimization problem:

$$\mathbf{p}^\star = \underset{\mathbf{p}}{\text{argmax}} \frac{\left(\mathbf{p}^T\hat{\mathbf{Q}}\mathbf{p}\right)^2}{\mathbf{p}^T\mathbf{p}\mathbf{p}^T\left(\mathbf{B}_I+\mathbf{B}_Z\right)\mathbf{p}+\left(\mathbf{p}^T\mathbf{p}\right)^2c}. \quad (4)$$

The optimization problem in (4) can be solved by numerical optimization using Matlab's *fminunc*. It is observed that different initial vectors lead to the same $\mathbf{p}^\star$.

V. Optimal integration window

In this section, we derive the integration window $\mathbf{g}^\star$ that maximizes the SINR of (2) for a given $\mathbf{p}^\star$. In order to find an analytic solution, the single terms in (2) are written in quadratic forms of $\mathbf{g}_{ext}$ in the following.

The squared interference term i_q is given by $i_q = \mathbf{g}_{ext}^T(\mathbf{i}\odot\mathbf{i})$. The variance of i_q can be calculated according to

$$\begin{aligned}\mathrm{E}_i\left\{i_q^2\right\} &= \mathbf{g}_{ext}^T\left(\mathrm{E}_i\left\{(\mathbf{i}\odot\mathbf{i})(\mathbf{i}\odot\mathbf{i})^T\right\}\right)\mathbf{g}_{ext}\\ &= 2\mathbf{g}_{ext}^T\left(\mathbf{R}_I\odot\mathbf{R}_I\right)\mathbf{g}_{ext}.\end{aligned}$$

The corresponding expression for the variance of z_q is obtained by replacing $\mathbf{R}_I$ with $\mathbf{R}_Z$.

The variance of i_s can be written as quadratic form in $\mathbf{g}_{ext}$ according to

$$\begin{aligned}\mathrm{E}_{h,i}\left\{i_s^2\right\} &= 4\mathbf{g}_{ext}^T\left(\mathrm{E}_{h,i}\left\{(\mathbf{H}\mathbf{p}^\star\odot\mathbf{i})(\mathbf{H}\mathbf{p}^\star\odot\mathbf{i})^T\right\}\right)\mathbf{g}_{ext}\\ &= 4\mathbf{g}_{ext}^T\left(\bar{\mathbf{Q}}\odot\mathbf{R}_I\right)\mathbf{g}_{ext}.\end{aligned}$$

The (i,j)-th element of $\bar{\mathbf{Q}}$ is given by $\bar{Q}_{i,j} = \mathbf{p}^{\star T}\mathrm{E}_h\left\{\mathbf{h}_i\mathbf{h}_j^T\right\}\mathbf{p}^\star$. Again, by replacing $\mathbf{R}_I$ with $\mathbf{R}_Z$, the variance for z_s is obtained. Finally, the variance of interference times noise $z_i = 2\mathbf{g}_{ext}^T(\mathbf{z}\odot\mathbf{i})$ is given by

$$\begin{aligned}\mathrm{E}_{i,z}\left\{z_i^2\right\} &= 4\mathbf{g}_{ext}^T\left(\mathrm{E}_{i,z}\left\{(\mathbf{z}\odot\mathbf{i})(\mathbf{z}\odot\mathbf{i})^T\right\}\right)\mathbf{g}_{ext}\\ &= 4\mathbf{g}_{ext}^T\left(\mathbf{R}_Z\odot\mathbf{R}_I\right)\mathbf{g}_{ext}.\end{aligned}$$

With these results and (3) the SINR from (2) can be written as Rayleigh Quotient in $\mathbf{g}_{ext}$ according to

$$\mathrm{SINR}\left(\mathbf{p}^\star,\mathbf{g}_{ext}\right) = \frac{\mathbf{g}_{ext}^T\mathbf{Q}\mathbf{g}_{ext}}{\mathbf{g}_{ext}^T\mathbf{B}\mathbf{g}_{ext}}, \quad (5)$$

where both matrices $\mathbf{Q}$ and $\mathbf{B}$ are symmetric, $\mathbf{Q}$ is positive semi-definite and $\mathbf{B}$ is positive definite given by

$$\mathbf{B} = \underbrace{2\left(\mathbf{R}_I\odot\mathbf{R}_I+\mathbf{R}_Z\odot\mathbf{R}_Z\right)}_{i_q+z_q} + \underbrace{4\bar{\mathbf{Q}}\odot\left(\mathbf{R}_I+\mathbf{R}_Z\right)}_{i_s+z_s} + \underbrace{4\mathbf{R}_Z\odot\mathbf{R}_I}_{z_i}.$$

Since the integration window of the energy detection receiver is given by $\mathbf{g}_{ext}^T = \left[\mathbf{g}^T, -\mathbf{g}^T\right]$, (5) can be reformulated as Rayleigh Quotient in $\mathbf{g}$ using matrices $\mathbf{C}$ and $\mathbf{U}$ with dimension $N_b/2\times N_b/2$, which are constructed according to

$$\begin{aligned}\mathbf{C} &= \mathbf{B}_{[1,\ldots,N_b/2],[1,\ldots,N_b/2]} + \mathbf{B}_{[N_b/2+1,\ldots,N_b],[N_b/2+1,\ldots,N_b]}\\ &\quad - \mathbf{B}_{[1,\ldots,N_b/2],[N_b/2+1,\ldots,N_b]} - \mathbf{B}_{[N_b/2+1,\ldots,N_b],[1,\ldots,N_b/2]},\\ \mathbf{U} &= \mathbf{Q}_{[1,\ldots,N_b/2],[1,\ldots,N_b/2]} + \mathbf{Q}_{[N_b/2+1,\ldots,N_b],[N_b/2+1,\ldots,N_b]}\\ &\quad - \mathbf{Q}_{[1,\ldots,N_b/2],[N_b/2+1,\ldots,N_b]} - \mathbf{Q}_{[N_b/2+1,\ldots,N_b],[1,\ldots,N_b/2]}.\end{aligned}$$

The eigenvector $\mathbf{g}^\star$ corresponding to the largest eigenvalue of $\mathbf{C}^{-1}\mathbf{U}$ maximizes (5).

VI. Performance Results

The investigated communication system uses the frequency band from 3 GHz to 4 GHz, which is determined by the 3 dB cutoff frequencies of the bandpass filter $h_{BP}[n]$. The bit duration is 40 ns and the duration of a PPM slot is 20 ns. This system would offer a data rate of 25 Mbps. The simulation sampling frequency is 20 GHz, which yields $N_b = 800$ and $N_{ppm} = 400$. The channel taps are modeled as zero-mean Gaussian with an exponentially decaying power delay profile. The maximum excess delay is set to 10 ns ($N_h = 200$) and the path loss to 55 dB. The center frequency and the bandwidth of the interference are set to 3.5 GHz and 20 MHz, respectively.

The average signal-to-noise and signal-to-interference ratio at the energy detector input are defined as

$$\mathrm{SNR_{IN}} = \frac{\mathrm{E}_h\left\{\frac{1}{N_b}\sum_{n=1}^{N_b}\left(p[n]*h[n]\right)^2\right\}}{R_Z[0]},$$

$$\mathrm{SIR_{IN}} = \frac{\mathrm{E}_h\left\{\frac{1}{N_b}\sum_{n=1}^{N_b}\left(p[n]*h[n]\right)^2\right\}}{R_I[0]}.$$

The $\mathrm{SNR_{IN}}$ is related to the ratio of the average receive energy per bit E_b over the noise power spectral density $N_0/2$ by E_b/N_0 [dB] = $\mathrm{SNR_{IN}}$ [dB] + 16.4 dB. Changing the transmit power of the UWB system and the power of the interference yields different $\mathrm{SNR_{IN}}$ and $\mathrm{SIR_{IN}}$ operating points. The optimal pulse shape and integration window depend on the current operating point of the system, since for different $\mathrm{SNR_{IN}}$ and $\mathrm{SIR_{IN}}$ values different terms in the denominator of (2) are dominating the overall performance.

A. Transmit Pulse Optimization

Fig. 2 shows one reference pulse and one optimized pulse for a rectangular integration window in frequency and time domain. The operating point is $\mathrm{SIR_{IN}} = 5$ dB and $\mathrm{SNR_{IN}} = 7.8$ dB, which corresponds to $E_b/N_0 = 24.2$ dB and a transmit power of -20.8 dBm. The reference pulse is obtained by solving the same optimization as in (4) without considering the interference. It can be seen that the optimized pulse has no significant spectral contribution, where the PSD of the interferer is non-zero. This means that the variance of the signal times interference term i_s is minimized (cf. [3],[4]). Fig. 3 depicts the BER performance of the reference pulse with and without interference, and the optimized pulses

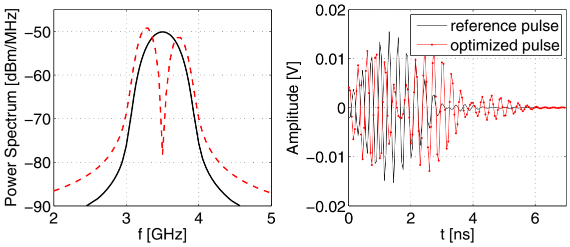

Fig. 2. Reference pulse and optimized pulse in frequency and time domain for $E_b/N_0 = 24.2$ dB and $\text{SIR}_{\text{IN}} = 5$ dB.

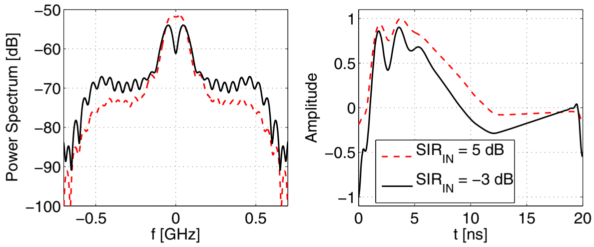

Fig. 4. Optimized window functions in frequency and time domain for $E_b/N_0 = 14.6$ dB and optimized pulse shapes.

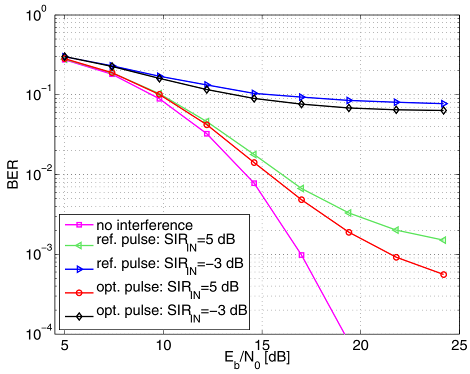

Fig. 3. BER for rectangular integration window.

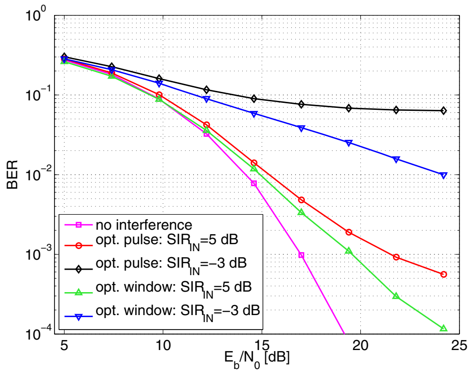

Fig. 5. BER for optimized integration windows.

with interference for a rectangular integration window. For low SIR_{IN} values the quadratic interference term i_q dominates the performance. This term cannot be influenced by the pulse shape, which explains the marginal performance gains for $\text{SIR}_{\text{IN}} = -3$ dB. For increasing SIR_{IN}, the dominance of i_q vanishes and the term i_s starts to be performance limiting for large E_b/N_0. For an SIR_{IN} of 5 dB, the BER can be reduced by a factor of three at $E_b/N_0 = 24.2$ dB.

B. Optimal Integration Window

Fig. 4 shows two exemplary windows for a fixed SNR_{IN} and two different values of SIR_{IN}. For low SIR_{IN} the window suppresses low frequencies from -20 to 20 MHz. This is exactly the frequency contribution of the squared interference signal around zero frequency. However, if the interference power is small, it can be seen that the window is matched to the power delay profile of the channel convolved with the transmit pulse shape. In Fig. 5 the performance curves for optimized pulse shapes and rectangular windows are compared with the performance curves for optimized pulse shapes and optimized windows. It can be seen that for $E_b/N_0 = 24.2$ dB, the BER can be further reduced by approximately a factor of six independent of SIR_{IN}. For increasing E_b/N_0 the BER approaches zero, which implies that interference can be fully suppressed.

VII. Conclusions

We have presented a theoretical framework, which allows to optimize pulse shapes and integration windows of energy detection receivers in the presence of interference and noise. Furthermore, statistical channel knowledge in form of the channel covariance matrix is incorporated into the cost function. If the covariance matrix is obtained by averaging over a confined geographic region, SNR gains can be expected.

The evaluation of the proposed interference mitigation scheme shows significant performance gains even for wideband interferers with 20 MHz bandwidth. The bandwidth of the interference plays an important role, since it determines, together with the SIR_{IN}, the dominance of squared interference i_q or signal times interference i_s contribution. The squared interference term becomes more and more negligible for smaller bandwidths (cf. [4]), which implies that pulse shaping becomes more effective for narrowband interference.

VIII. Acknowledgements

The work presented in this paper was partially supported by the National Competence Center in Research on Mobile Information and Communication Systems (NCCR-MICS), a center supported by the Swiss National Science Foundation under grant number 5005-67322.

References

[1] L. Yang and G. B. Giannakis, "Ultra-wideband communications: An idea whose time has come," *IEEE Signal Processing Magazine*, vol. 21, no. 6, pp. 26–54, Nov. 2004.

[2] H. Arslan and M. E. Shin, *Cognitive Radio, Software Defined Radio, and Adaptive Wireless Systems*. Springer Netherlands, 2007.

[3] X. Luo, L. Yang, and G. Giannakis, "Designing optimal pulse-shapers for ultra-wideband radios," *Journal on Communications and Networks*, vol. 5, no. 4, pp. 344–353, December 2003.

[4] C. Steiner and A. Wittneben, "On the interference robustness of ultra-wideband energy detection receivers," *IEEE International Conference on Ultra-Wideband, ICUWB 2007*, pp. 721–726, September 2007.

[5] Y. Alemseged and K. Witrisal, "Energy detection under narrowband interference in UWB systems," *6th International Conference on Information, Communications and Signal Processing*, Dec. 2007.